Fault detection of a benchmark wind turbine using interval analysis

Tabatabaeipour, Seyed Mojtaba; Odgaard, Peter Fogh; Bak, Thomas

Published in:
2012 American Control Conference (ACC)

Publication date:
2012

Document Version
Publisher's PDF, also known as Version of record

2012 American Control Conference
Fairmont Queen Elizabeth, Montréal, Canada
June 27-June 29, 2012

Fault detection of a benchmark wind turbine using interval analysis

Seyed Mojtaba Tabatabaeipour and Peter F. Odgaard, and Thomas Bak

Abstract— **This paper investigates a state estimation set-membership approach for fault detection of a benchmark wind turbine. The main challenges in the benchmark are high noise on the wind speed measurement and the nonlinearities in the aerodynamic torque such that the overall model of the turbine is nonlinear. We use an effective wind speed estimator to estimate the effective wind speed and then using interval analysis and monotonicity of the aerodynamic torque with respect to the effective wind speed, we can apply the method to the nonlinear system. The fault detection algorithm checks the consistency of the measurement with a closed set that is computed based on the past measurements and a model of the system. If the measurement is not consistent with this set, a fault is detected. The result demonstrates effectiveness of the method for fault detection of the benchmark wind turbine.**

I. INTRODUCTION

In recent years, there is an increasing attention to wind energy as one of the most promising and abundant sources for sustainable energy. But, the installation and maintenance cost of wind turbines are very high. This is more critical for an offshore wind turbine. Like every other systems, wind turbines are prone to faults. The control system is of high importance for detection, isolation and accommodation of faults in wind turbines since it has access to information from the different components in the wind turbine. For an offshore wind turbine, a non-planned service is very expensive. Therefore, it is important to design a control system that can automatically detect and isolate occurred faults, maintain the overall functionality of the wind turbine, and provide an acceptable performance for the faulty system without an unnecessary need to shut down the system.

In recent years there has been some works investigating the problem of fault diagnosis and fault tolerant control of wind turbines, see [1]. [2] proposes an observer based fault detection for detecting sensor faults in the pitch system. An unknown input observer is used in [3] for sensor fault detection in the drive train. [4] investigates fault detection and fault tolerant control of the electrical conversion systems.

A benchmark model for fault detection, isolation and accommodation of wind turbines was proposed in [5]. The benchmark is based on the model of a generic three blade horizontal variable speed wind turbine with a full converter coupling and a rated power of 4.8 MW. The aim of the benchmark model is to provide a common ground to test and compare different methods for fault detection and accommodation of wind turbines. Recently a number of papers have been published on fault detection and isolation of the benchmark proposed in [5]. In [6] a solution based on Kalman filters and diagnositic observers for residual generation with generalized likelihood ratio test for detection decision is proposed. Solutions based on support vector machines are proposed in [7]. In [8] a model based method is used to generate residuals on which an up-down counter based scheme is used for detection and isolation. [9] presents a generic automated design method for fault detection and isolation on this benchmark. A scheme based on fault detection and isolation estimators is proposed in [10]. In [11] a set-theoretic method is proposed for this problem. [12] focuses on generalized likelihood ratio and associated statistical fault detection tools. A hybrid approach is taken in [13]. In [14] a data driven approach is taken on the benchmark model. In [15] a detection and isolation scheme based on a combination of parity equations and robust residual filterings is proposed.

In this paper we investigate application and adaptation of the state space based set-membership fault detection method for fault detection of the benchmark model. In real applications, there are always noise, uncertainties and model differences. To ensure reliability and performance of a fault detection method, it must be insensitive to uncertainties and noise but sensitive to faults. A fault detection method with this property is called robust. There are two main approaches to robust fault detection: active and passive. In the robust active fault detection, fault detection is based on the value of a residual signal. If the value of the residual signal is bigger than a threshold a fault is detected. The challenge is to generate a residual signal which is sensitive to faults and insensitive to noise and uncertainties. Amongst active approaches are unknown input observers [16], eigenstructure assignment [17], and structured parity equations [18].

In the passive approach, the noise, disturbance and uncertainties on the parameters of the model are assumed to be unknown but bounded with a priori known bound. Then, a set of models is generated for the system. A fault is detected if a measurement is not consistent with any member of this set. In the control literature these approaches are known as set-membership, or error bounded methods, see [19], [20] for a review. An advantage of the set-membership approach is that there is no need for a threshold design. A fault is detected if the estimated states or the estimated parameters are outside a closed set. Another advantage is that, if the given bounds on the uncertainties, noise and disturbance are realistic, no positive false alarm is generated. The drawback of the method is its conservatism because uncertainties are propagated. Set-membership approaches can be divided into two categories: state estimation based and parameter

S. M. Tabatabaeipour and T. Bak are with Automation & Control, Department of Electronic Systems, Aalborg University, DK-9220, Denmark. smt@es.aau.dk

P. F Odgaard is with kk-electronic a/s, 7430 lkast, Denmark, (+45 21744963). peodg@kk-electronic.com

estimation based. The idea is to estimate the set of states or parameters that are consistent with the measurements. If a measurement can not be explained by this set, then a fault is detected.

All of the aforementioned methods for fault detection of the benchmark are active. In [21] a passive robust approach is proposed which investigates application of the parameter estimation based method for fault detection of wind turbines. But they assume that the system can be represented by a model that is linear in the estimated parameters. In this work, we use the state estimation set-membership method using the nonlinear model of the system. The nonlinear term is approximated by an interval at each sample time. While [21] cannot detect fault no. 6 in the benchmark, we can detect this fault, also other faults are detected at the same time or sooner than the reported results in [21].

The paper is organized as follows. In section 2, the benchmark model and fault scenarios are explained. In section 3, the state space set-membership approach is given and it is explained how we deal with the nonlinear term. Simulation results and discussion are given in section 5. Finally, section 6 concludes the paper.

A. Basic Nomenclature and Definitions

A closed interval $[a] = [\underline{a}, \overline{a}]$ is the set $[\underline{a}, \overline{a}] = \{x \in \mathbb{R} : \underline{a} \leq x \leq \overline{a}\}$. Basic arithmetic operation are defined between intervals [22]. For the operation $\odot \in \{+; -; \times; /\}$ and two intervals $[a]$ and $[b]$, $[a] \odot [b]$ is defined as:$[a] \odot [b] = \{x \odot y : x \in [a], y \in [b]\}$. An n-dimensional box $[\mathbf{x}]$ is a vector interval which is an ordered n-tuple of intervals $([x_1], [x_2], \cdots, [x_n])$. The range of the function f over the interval vector $[x]$ is defined by $f([x]) = \{f(x) : x \in [x]\}$. If f is a monotonic function, then $f([x]) = [f(\underline{x}), f(\overline{x})]$. Given two sets $\mathscr{X} \in \mathbb{R}^n$ and $\mathscr{Y} \in \mathbb{R}^n$, the Minkowski sum of them is defined as $\mathscr{X} \oplus \mathscr{Y} = \{x+y : x \in \mathscr{X}, y \in \mathscr{Y}\}$.

II. Wind turbine description

The benchmark model presents a model of a generic three blade horizontal axis turbine with a full converter. Figure 1 depicts the block diagram of the wind turbine. The wind turbine model consists of four parts: blade and pitch systems, drive train, generator and convertor, and the controller. The wind energy is transformed to mechanical energy through rotation of the blades by the wind. By pitching the blades or by controlling the rotational speed of the turbine relative to the wind speed, we can change aerodynamics of the turbine and hence we can control this mechanical energy. The generator which is fully coupled with a convertor transforms the mechanical energy to electrical energy. The role of the drive train is to increase the rotational speed from the rotor to the generator. The generator torque can be controlled by the convertor. Using the generator torque, the rotational speed of the generator or the rotor can be controlled. The rotor speed, the generator speed, and the pitch positions of all blades are measured with two sensors. In the following, different subsystems are described in more detail.

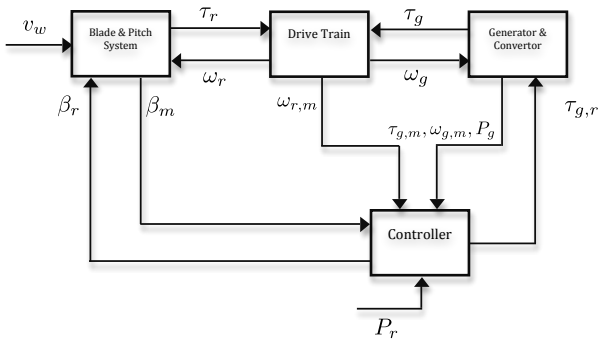

Fig. 1. Block diagram of the wind turbine model

A. Blade and pitch system

This model is comprised of two parts: the aerodynamic model and the pitch model.

Aerodynamic Model

The aerodynamic torque applied to the rotor is modeled as:

$$\tau_r(t) = \frac{1}{2}\rho\pi R^3 C_q(\lambda(t), \beta(t)) v_w^2, \tag{1}$$

where C_q is the torque coefficient which is a function of the pitch angle, β and the ration between the speed of the blade tip and the wind speed known as the tip-speed ratio given by:

$$\lambda(t) = \frac{R\omega_r(t)}{v_w(t)}, \tag{2}$$

where R is the radius of the blades and v_w is the wind speed and ω_r is the rotor speed. C_q is given in the form of a look-up table. In case the blades might have different pitch angles, a simple way to model the aerodynamic torque is:

$$\tau_r(t) = \Sigma_{i=1}^{3} \frac{1}{6}\rho\pi R^3 C_q(\lambda(t), \beta_i(t)) v_w^2. \tag{3}$$

Pitch System Model

The pitch system considered in this model is a hydraulic pitch system. The closed loop dynamic of the pitch system is described by a second-order system:

$$\frac{\beta(s)}{\beta_r(s)} = \frac{\omega_n^2}{s^2 + 2\xi\omega_n s + \omega_n^2}, \tag{4}$$

where β_r is the pitch reference.

B. Drive Train Model

The drive train is modeled as an interconnection of a low speed shaft and a high-speed shaft which are interconnected through a transmission with a gear ration of N_g. The drive train dynamic is modeled by the following system:

$$\begin{bmatrix} \dot{\omega}_r(t) \\ \dot{\omega}_g(t) \\ \dot{\theta}_\Delta(t) \end{bmatrix} = A_{DT} \begin{bmatrix} \omega_r(t) \\ \omega_g(t) \\ \theta_\Delta(t) \end{bmatrix} + B_{DT} \begin{bmatrix} \tau_r(t) \\ \tau_g(t) \end{bmatrix}, \tag{5}$$

where

$$A_{DT} = \begin{bmatrix} -\frac{B_{dt}+B_r}{J_r} & \frac{B_{dt}}{N_g J_r} & -\frac{K_{dt}}{J_r} \\ \frac{\eta_{dt} B_{dt}}{N_g J_g} & \frac{-\frac{\eta_{dt} B_{dt}}{N_g^2} - B_g}{J_g} & \frac{\eta_{dt} K_{dt}}{N_g J_g} \\ 1 & -\frac{1}{N_g} & 0 \end{bmatrix}, \quad (6)$$

$$B_{DT} = \begin{bmatrix} \frac{1}{J_r} & 0 \\ 0 & -\frac{1}{J_g} \\ 0 & 0 \end{bmatrix}, \quad (7)$$

where J_g denotes the moment inertia of the low-speed shaft, K_{dt} denotes the torsion stiffness of the drive train, B_{dt} is the torsion damping coefficient of the drive train, B_g is the viscous friction of the high speed shaft. Ω_g is the rotational speed of the generator, the moment of inertia of the high-speed shaft is denoted by J_g, the efficiency of the drive train is denoted by η_{dt}, and the torsion angle of it is denoted by $\theta_\Delta(t)$.

C. Generator and Convertor Models

The generator torque is controlled by a reference $\tau_{g,r}$. The dynamic of the convertor is approximated by a first order system as:

$$\frac{\tau_g(s)}{\tau_{g,r}(s)} = \frac{\alpha_{gc}}{s+\alpha_{gc}}. \quad (8)$$

The produced power by the generator is given by:

$$P_g(t) = \eta_g \omega_g(t) \tau_g(t), \quad (9)$$

where η_g is the efficiency of the generator. Model parameters can be found in [5].

D. fault scenarios

The following types of fault are considered in the benchmark: sensor faults, actuator faults, and system faults.

Sensor Faults

Sensor faults and their description are summarized in table I where index *mi* represent the $i'th$ measurement of the corresponding variable.

TABLE I
LIST OF SENSOR FAULTS

Fault No.	Fault	period	Description
1	$\beta_{1,m_1} = 5^\circ$	2000-2100	Pitch sensor fixed value
2	$\beta_{1,m_2} = 1.2\beta_{1,m_2}$	2300-2400	Pitch sensor gain factor
3	$\beta_{3,m_1} = 10^\circ$	2600-2700	Pitch sensor fixed value
4	$\omega_{r,m_1} = 1.4$ rad/s	1500-1600	Rotor speed fixed value
5	$\omega_{r,m_2} = 1.1\omega_{r,m_2}$ $\omega_{g,m_1} = 0.9\omega_{g,m_1}$	1000-1100	Rotor and generator speed gain factor

Actuator Faults

Two kinds of actuator faults are considered for the pitch system. The first fault is a hydraulic pressure drop in actuator 2. The pressure drop is modeled as an abrupt change of parameters of the pitch system from ω_n, ξ to ω_{n2}, ξ_2. The second fault is an air content increase in the actuator oil. This fault is modeled as a gradual change in the parameters of the pitch actuator 3. The parameter are changed linearly from ω_n, ξ to ω_{n3}, ξ_3 in a period of 30 s, they remain active for 40s, and decrease again for 30s. Actuator faults are summarized in table II

TABLE II
LIST OF ACTUATOR FAULTS

Fault No.	Fault	period	Description
6	abrupt change of $\omega_n, \xi \to \omega_{n2}, \xi_2$	2900-3000	Pressure drop
7	slow change of $\omega_n, \xi \to \omega_{n3}, \xi_3$	3400-3500	air content increase in the oil

System Faults

A system fault is considered in the benchmark. The system fault is a bias in the generator control loop which yields a bias in the generator torque: $\tau_g = \tau_g + 2000Nm$.

TABLE III
SYSTEM FAULT

Fault No.	Fault	period	Description
8	$\tau_g = \tau_g + 2000Nm$	3800-3900	Offset

III. STATE SPACE SET-MEMBERSHIP FAULT DETECTION

Consider the following nonlinear model:

$$x(k+1) = f(x(k), u(k), w(k)), \quad (10)$$

$$y(k) = g(x(k), v(k)), \quad (11)$$

where $x(k) \in \mathbb{R}^n$ is the state, $y(k) \in \mathbb{R}^m$ is the output, $u(k) \in \mathbb{R}^p$ is the input, $w(k) \in \mathbb{R}^n$ is disturbance and $v(k) \in \mathbb{R}^m$ is noise. We assume that the noise and disturbance are unknown but bounded i.e. $w(k) \in \mathscr{W}$ and $v(k) \in \mathscr{V}$. Moreover, we assume that the initial condition is given in a compact set $x(0) \in \mathscr{X}_0$.

The set-membership approach uses the consistency principle for fault detection. At each iteration, given the model of the system, the initial condition set and bounds on the disturbance and noise, the set of all states that are consistent with the sequence of input-output up to the current sample time, $\mathbb{X}^c(k)$ is computed. A fault is detected if this set is empty. Computation of $\mathbb{X}^c(k)$ consist of two steps: a prediction step and a correction step. At the prediction step, having $\mathbb{X}^c(k-1)$, the predicted set $\mathbb{X}^p(k)$ is defined as:

$$\mathbb{X}^p(k) = \{f(x(k-1), u(k-1), w(k-1)) : x(k-1) \in \mathbb{X}^c(k-1), u(k-1) = u(k-1), w(k-1) \in \mathscr{W}\}. \quad (12)$$

The predicted set is one-step ahead prediction of $\mathbb{X}^c(k-1)$. This set can be corrected using the information provided by the current output y(k). Let us define $\mathbb{X}^y(k)$ as the set of all states that are consistent with $y(k)$:

$$\mathbb{X}^y(k) = \{x \in \mathbb{R}^n : \exists v \in \mathscr{V} \text{ such that } g(x,v) = y(k)\}. \quad (13)$$

When noise is additive i.e. $g(x,v) = h(x) + v$, then:

$$\mathbb{X}^y(k) = \{x : h(x) \in y(k) \oplus (-V)\}. \quad (14)$$

Then, the corrected set is defined as:

$$\mathbb{X}^c(k) = \mathbb{X}^p(k) \cap \mathbb{X}^y(k). \quad (15)$$

TABLE IV

STATE SPACE SET-MEMBERSHIP FAULT DETECTION

Algorithm 1
Given $f, g, \mathscr{X}_0, \mathscr{V}, \mathscr{W}$
$k=0$, Fault $\leftarrow$ False, $\mathbb{X}^c(k)=\mathscr{X}_0$
While Fault=False $k=k+1$
Given $u(k)$, find the prediction set:
$\mathbb{X}^p(k)=\{f(x(k-1),u(k-1),w(k-1)) : x(k-1)\in\mathbb{X}^c(k-1),$
$u(k-1)=u(k-1), w(k-1)\in\mathscr{W}\}$.
Given $y(k)$, find $\mathbb{X}^y(k)$:
$\mathbb{X}^y(k)=\{x\in\mathbb{R}^n : \exists v\in\mathscr{V}, g(x,v)=y(k)\}$.
$\mathbb{X}^c(k)=\mathbb{X}^p(k)\cap\mathbb{X}^y(k)$
If $\mathbb{X}^c(k)=\emptyset$, then Fault=True
end

A fault is detected if

$$\mathbb{X}^p(k)\cap\mathbb{X}^y(k)=\emptyset. \tag{16}$$

The overall algorithm for fault detection is given in table IV.

Exact computation of these sets using the general nonlinear model is very difficult. Therefore, in the literature some simplifying assumptions about the nonlinear model is made. Also, the sets are over-approximated by ellipsoids, polyhedrons, parallelotopes, intervals, or zonotopes, see [23] and references therein. The benefit of using ellipsoidal set is their simplicity. In this work, we use polytopes for bounding of the states. The advantage of polytopes is that the accuracy of estimation is increased and the drawback is higher computational complexity.

A. Fault detection of the wind turbine

The model of the wind turbine is summarized as follows:

$$x(k+1)=\begin{bmatrix}\omega_r(k+1)\\ \omega_g(k+1)\\ \theta_\Delta(k+1)\\ \tau_g(k+1)\\ \beta(k+1)\\ \beta(k+2)\end{bmatrix}=A\begin{bmatrix}\omega_r(k)\\ \omega_g(k)\\ \theta_\Delta(k)\\ \tau_g(k)\\ \beta(k)\\ \beta(k+1)\end{bmatrix}$$
$$+B\begin{bmatrix}\tau_{g,r}(k) & \beta_r(k)\end{bmatrix}^T+B_{\tau_r}\tau_r(k), \tag{17}$$

$$y(k)=\begin{bmatrix}1&0&0&0&0_{1\times3}&0_{1\times3}\\ 0&1&0&0&0_{1\times3}&0_{1\times3}\\ 0&0&0&1&0_{1\times3}&0_{1\times3}\\ 0_{3\times1}&0_{3\times1}&0_{3\times1}&0_{3\times1}&I_{3\times3}&0_{3\times3}\end{bmatrix}x_{dc}(k)+v, \tag{18}$$

where A and B are produced by an appropriate augmentation of the corresponding matrices of the drive train, the generator and the pitch system. Assume that at $k-1$, we have $\mathbb{X}^c(k-1)$. Then, we use (17) to find $\mathbb{X}^p(k)$. If we can find an interval approximation of $\tau_r(k)$, then we have:

$$\mathbb{X}(k)^p=A\mathbb{X}^c(k-1)\oplus B\tau_{g,r}(k-1)\oplus B_{\tau_r}[\tau_r(k-1)]. \tag{19}$$

Moreover, having the measurement $y(k)$ and assuming that $\mathscr{V}$ is given as the box $\mathscr{V}=([v_{\omega_r}],[v_{\omega_g}],[v_{\tau_r}],[v_{\beta_1}],[v_{\beta_2}],[v_{\beta_3}])$, then the set $[x(k)]^y$ is obtained as:

$$\begin{aligned}[x(k)]^y=\{&\omega_r(k)+\underline{v}_{\omega_r}\le\omega_r\le\omega_r(k)+\overline{v}_{\omega_r},\\ &\omega_g(k)+\underline{v}_{\omega_g}\le\omega_g\le\omega_g(k)+\overline{v}_{\omega_g}\\ &\tau_g(k)+\underline{v}_{\tau_g}\le\tau_g\le\tau_g(k)+\overline{v}_{\tau_g}\\ &\{\beta_i(k)+\underline{v}_{\beta_i}\le\beta_i\le\beta_i(k)+\overline{v}_{\beta_i}\}_{i=1}^3\}\end{aligned} \tag{20}$$

The next problem is to find an interval approximation of $\tau_r(k)$ as $[\tau_r(k)]=[\underline{\tau}_r(k),\overline{\tau}_r(k)]$. Using interval analysis we have:

$$\overline{\tau}_r(k)=\Sigma_{i=1}^3\frac{1}{6}\rho\pi\overline{C_{qi}}(k)\overline{v}_w^2(k) \tag{21}$$

$$\underline{\tau}_r(k)=\Sigma_{i=1}^3\frac{1}{6}\rho\pi\underline{C_{qi}}(k)\underline{v}_w^2(k) \tag{22}$$

C_q is given in the form of a look-up table as a function of λ and β. We have $[\lambda(k)]=[\underline{\lambda}(k),\overline{\lambda}(k)]=[\frac{R\underline{\omega}_r}{\overline{v}_w},\frac{R\overline{\omega}_r}{\underline{v}_w}]$ and $[\beta_i]$ is computed using a set-membership observer for the pitch system. Then:

$$\overline{C_{qi}}=max(C_q([\lambda(k)],[\beta_i(k)])) \tag{23}$$

$$\underline{C_{qi}}=min(C_q([\lambda(k)],[\beta_i(k)])) \tag{24}$$

Note that using this method the uncertainties on the C_q table can also be handled easily. In order to find $[v_w]$, we need a bound on the measurement noise for the wind speed. The wind speed measurement has a high level of noise and there is a possibility of offset on this sensor. Therefore, using the information from this sensor would result in a very conservative over-approximation of $[\tau_r]$ which in turn would yield a poor performance of the fault detection algorithm. To address this problem we use an estimation of the effective wind speed instead of the measurement form the hub.

There are different methods to estimate effective wind speed, see [24] and [25]. In this work we use the method suggested in [24]. The proposed wind speed estimator consists of three parts: a state estimator, an input estimator and a look-up table. The state estimator estimates the states of the drive train. The input estimator which is a PI controller estimates the aerodynamic torque which is fed to the state estimator. Estimations of the rotor speed, the pitch angle from the state estimator and the aerodynamic torque are used as input to the look-up table to calculate the effective wind speed. The block diagram of the effective wind speed estimator is shown in Figure 2. We assume a bound on the estimation error of the EWS denoted by e_{v_w}. Figure 3 shows the interval approximation of the aerodynamic torque using EWS estimation and its real value for the time period $400s-900s$.

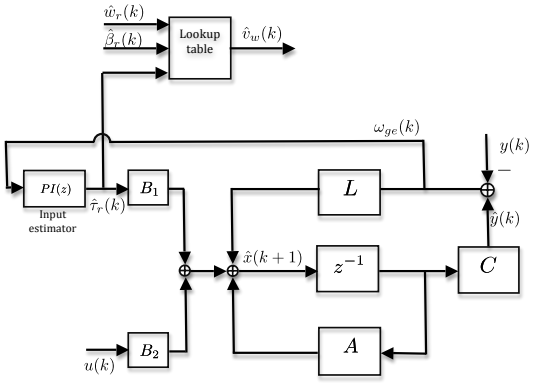

Fig. 2. Block diagram of the effective wind speed estimator

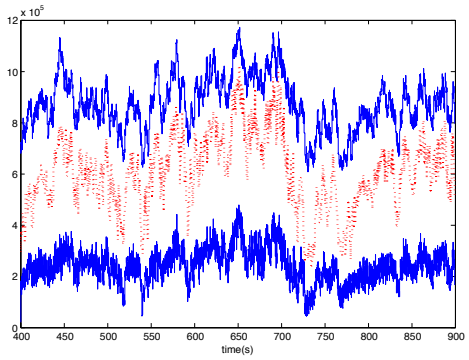

Fig. 3. Interval approximation of τ_r: τ_r dotted line, $\overline{\tau_r}, \underline{\tau_r}$: dashed line

TABLE V

STATE SPACE SET-MEMBERSHIP FAULT DETECTION

Algorithm 2
Given $A, B, \mathscr{X}_0, \mathscr{V}, e_{v_w}$
$k=1$, Fault $\leftarrow$ False, $\mathbb{X}^p(k)=\mathscr{X}_0$
While Fault=False
  Get input-output data $\{u(k), y(k)\}$
  Find $\mathbb{X}^y(k)$ using (20)
  $\mathbb{X}^c(k)=\mathbb{X}^y(k)\cap\mathbb{X}^p(k)$
  Get $v_w(k)$ from EWS estimator
  $\overline{v_w}(k)=v_w(k)+e_{v_w}, \underline{v_w}(k)=v_w(k)-e_{v_w}$
  $[\lambda(k)]=[\frac{R\omega_r(k)}{\overline{v_w}(k)}, \frac{R\omega_r(k)}{\underline{v_w}(k)}]$
  $\overline{C_{qi}}=max(C_q([\lambda(k)],[\beta_i(k)]))$
  $\underline{C_{qi}}=min(C_q([\lambda(k)],[\beta_i(k)]))$
  $\overline{\tau_r}(k)=\Sigma_{i=1}^{3}\frac{1}{6}\rho\pi\overline{C_{qi}}(k)\overline{v}_w^2(k)$
  $\underline{\tau_r}(k)=\Sigma_{i=1}^{3}\frac{1}{6}\rho\pi\underline{C_{qi}}(k)\underline{v}_w^2(k)$
  $[\tau_r(k)]=[\underline{\tau_r}(k), \overline{\tau_r}(k)]$
  $\mathbb{X}^p(k+1)=A\mathbb{X}^c(k)\oplus Bu(k)\oplus B_{\tau_r}[\tau_r(k)]$
  $\mathbb{X}^p(k+1)\leftarrow\square\mathbb{X}^p(k+1)$
  If $\mathbb{X}^c(k)=\emptyset$, then Fault=True
end

The overall algorithm for fault detection is given in table V. To avoid computational complexity, at each step k, $\mathbb{X}^p(k+1)$ can be over approximated by a bounding set using parallelotopes or zonotopes which is denoted by $\square\mathbb{X}^p(k+1)$.

IV. SIMULATION RESULTS

In this section simulation results of the proposed algorithm for fault detection of the benchmark are given. The sampling time is chosen to be $0.01s$. A discrete-time model of the system is obtained using zero order hold discretization method. The proposed algorithm assumes that noise in unknown but bounded but in the Simulink model of the benchmark, sensor noises are considered to be gaussian and hence theoretically unbounded. It is known that for a gaussian noise, if one chooses -6σ and 6σ band, the noise will be in the band with the probability of 99.99. Here, we use $\pm 10\sigma$ for the bound on the noise in our algorithm.

1) Fault 1: ($\beta_{1,m_1}=5^\circ$) Figure 4 shows the simulation result for detection of fault 1. In this figure diamonds represent the measurement, circles represent the consistent interval values of β_1 with the current measurement, i.e. $[\beta_1(k)]^y$, boxes represent the interval of the predicted set i.e $[\beta_1(k)]^p$, and crosses represent $[\beta_1(k)]^c$. As it can be seen right after the occurrence of the fault, $[\beta_1(k)]^p$ and $[\beta_1(k)]^y$ do not intersect which means $[\beta_1(k)]^c$ is empty and the fault is detected. We have done multiple of simulations and there was no positive false alarm.

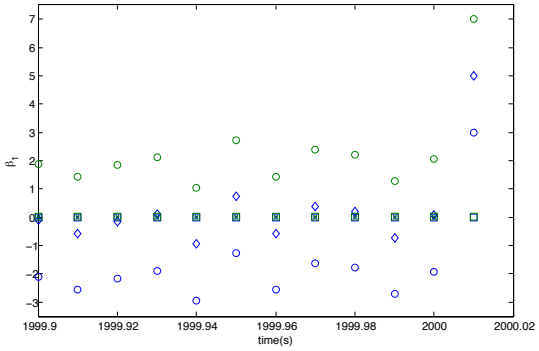

Fig. 4. Detection of fault 1,$\diamond$: current measurement $\beta_{1,m}(k)$, $\circ$: $[\beta_1(k)]^y$, $\square$:$[\beta_1(k)]^p$, $\times$: $[\beta_1(k)]^c$

2) Fault 2: ($\beta_{1,m_2}=1.2\beta_{1,m_2}$) Due to the high level of noise on the pitch measurement, it takes some time to detect the fault. The fault is detected at $2307.41s$. If we uses $v_\beta=8\sigma$ band, then the fault is detected at $2304.21s$.

3) Fault 3: ($\beta_{3,m_1}=10^\circ$) This fault is detected within one sample. The result is shown in figure 5

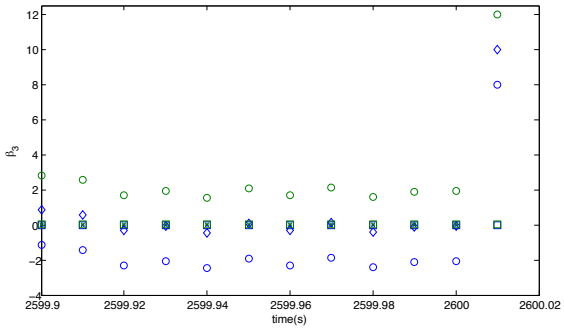

Fig. 5. Detection of fault 3,$\diamond$: current measurement $\beta_{3,m}(k)$, $\circ$: $[\beta_3(k)]^y$, $\square$:$[\beta_3(k)]^p$, $\times$: $[\beta_3(k)]^c$

4) Fault 4: ($\omega_{r,m_1}=1.4$rad/s) Due to high level of noise on this measurement, we first filter the measurement and then apply the method. This would cause a delay in the detection and the fault is detected in 5 samples. Figure 6 shows the result of fault detection.

5) Fault 5: ($\omega_{r,m_2}=1.1\omega_{r,m_2}, \omega_{g,m_1}=0.9\omega_{g,m_1}$) The fault is detected in 1 sample time.

6) Fault 6: (abrupt change of $\omega_n, \xi\rightarrow\omega_{n2}, \xi_2$) Detection of this fault is not possible until there is some enough big changes in the pitch reference signal which is zero for about 50 seconds after fault occurrence. The fault is detected at 2951.69.

7) Fault 7: (gradual change of $\omega_n, \xi\rightarrow\omega_{n3}, \xi_3$) The fault is detected at 3424.83 choosing v_β to be $10\sigma_\beta$.

8) Fault 8: ($\tau_g=\tau_g+2000Nm$) The fault is detected in one sample.

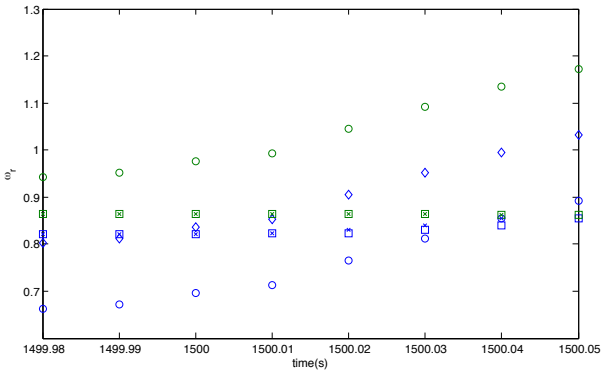

Fig. 6. Detection of fault 4,◇: current measurement $\omega_{r,m_1}(k)$, ○: $[\omega_{r,m_1}(k)]^y$, □:$[\omega_{r,m_1}(k)]^p$, ×: $[\omega_{r,m_1}(k)]^c$

The results are summarized in table VI, where T_f is the occurrence time and T_D is the detection time of a fault.

TABLE VI
SUMMARY OF FAULT DETECTION RESULTS

Fault No.	T_f	T_D
1	2000s	2000.01s
2	2300s	2304.21s
3	2600s	2600.01s
4	1500s	1500.05s
5	1000s	1000.01s
6	2900s	2951.69s
7	3400s	3424.83s
8	3800s	3800.01s

V. CONCLUSIONS AND FUTURE WORKS

A method for fault detection of a benchmark wind turbine which includes sensor, actuator and system faults is proposed. The method is based on the state space set-membership consistency test. Instead of using wind speed measurement, we use effective wind speed estimation and then using interval analysis, the aerodynamic torque which is nonlinear is over-approximated by an interval . The simulation results show that we can detect all of the proposed faults including fault no.6 that was not detected in the other proposed passive approach; moreover most of the faults are detected faster.

VI. ACKNOWLEDGMENTS

This work is supported by Norwegian research center for wind energy.

REFERENCES

[1] T. Esbensen and C. Sloth, "Fault dangosis and fault-tolerant control of wind turbines," Master's thesis, Aalborg University, 2009.

[2] X. Wei, M. Verhaegen, and T. van den Engelen, "Sensor fault diagnosis of wind turbines for fault tolerant," in *Proceedings of the 17th World Congress The International Federation of Automatic Control*, 2009, pp. 3222–3227.

[3] P. Odgaard and J. Stoustrup, "Unknown input observer based detection of sensor faults in a wind turbine," in *Control Applications (CCA), 2010 IEEE International Conference on*, sept. 2010, pp. 310 –315.

[4] P. Poure, P. Weber, D. Theilliol, and S. Saadate, "Fault-tolerant power electronic converters: Reliability analysis of active power filter," in *IEEE International Symposium on Industrial Electronics*. IEEE, 2007, pp. 3174–3179.

[5] P. Odgaard, J. Stoustrup, and M. Kinnaert, "Fault tolerant control of wind turbines a benchmark model," in *Proceedings of the 7th IFAC Symposium on Fault Detection, Supervision and Safety of Technical Processes*. Barcelona, Spain: IFAC, June-July 2009, pp. 155–160.

[6] W. Chen, S. Ding, A. Sari, A. Naik, A. Khan, and S. Yin, "Observer-based fdi schemes for wind turbine benchmark," in *Proceedings of IFAC World Congress 2011*, Milan, Italy, August-September 2011, pp. 7073–7078.

[7] N. Laouti, N. Sheibat-Othman, and S. Othman, "Support vector machines for fault detection in wind turbines," in *Proceedings of IFAC World Congress 2011*, Milan, Italy, August-September 2011, pp. 7067–7072.

[8] A. Ozdemir, P. Seiler, and G. Balas, "Wind turbine fault detection using counter-based residual thresholding," in *Proceedings of IFAC World Congress 2011*, Milan, Italy, August-September 2011, pp. 8289–8294.

[9] C. Svard and M. Nyberg, "Automated design of an fdi-system for the wind turbine benchmark," in *Proceedings of IFAC World Congress 2011*, Milan, Italy, August-September 2011, pp. 8307–8315.

[10] X. Zhang, Q. Zhang, S. Zhao, R. M. Ferrari, M. M. Polycarpou, and T. Parisini, "Fault detection and isolation of the wind turbine benchmark: An estimation-based approach," in *Proceedings of IFAC World Congress 2011*, Milan, Italy, August-Septemper 2011, pp. 8295–8300.

[11] F. Stoican, C.-F. Raduinea, and S. Olaru, "Adaptation of set theoretic methods to the fault detection of wind turbine benchmark," in *Proceedings of IFAC World Congress 2011*, Milan, Italy, August-September 2011, pp. 8322–8327.

[12] F. Kiasi, J. Prakash, S. Shah, and J. Lee, "Fault detection and isolation of benchmark wind turbine using the likelihood ratio test," in *Proceedings of IFAC World Congress 2011*, Milan, Italy, August-September 2011, pp. 7079–7085.

[13] S. Simani, P. Castaldi, and M. Bonfe, "Hybrid modelbased fault detection of wind turbine sensors," in *Proceedings of IFAC World Congress 2011*, Milan, Italy, August-September 2011, pp. 7061–7066.

[14] S. Simani, P. Castaldi, and A. Tilli, "Datadriven approach for wind turbine actuator and sensor fault detection and isolation," in *Proceedings of IFAC World Congress 2011*, Milan, Italy, August-September 2011, pp. 8301–8306.

[15] B. Ayalew and P. Pisu, "Robust fault diagnosis for a horizontal axis wind turbine," in *Proceedings of IFAC World Congress 2011*, Milan, Italy, August- September 2011, pp. 7055–7060.

[16] J. Chen and R. Patton, *Robust model-based fault diagnosis for dynamic systems*. Kluwer academic publishers, 1999.

[17] R. Patton and J. Chen, "Robust fault detection of jet engine sensor systems using eigenstructure assignment," in *AIAA Guidance, Navigation and Control Conference, New Orleans, LA*, 1991, pp. 1666–1675.

[18] ——, "A review of parity space approaches to fault diagnosis." in . *IFAC SAFEPROCESS Symp.*, 1991, pp. 65–81.

[19] V. Puig, "Fault diagnosis and fault tolerant control using set-membership approaches: application to real case studies," *Internationl Journal of applied mathematics and computer sicence*, vol. 20, pp. 619–635, 2010.

[20] A. Ingimundarson, J. M. Bravo, V. Puig, T. Alamo, and P. Guerra, "Robust fault detection using zonotope-based set-membership consistency test," *International Journal of Adaptive Control and Signal Processing*, vol. 23, no. 4, pp. 311–330, 2009. [Online]. Available: http://dx.doi.org/10.1002/acs.1038

[21] J. Blesa, V. Puig, J. Romera, and J. Saludes, "Fault diagnosis of wind turbines using a set-membership approach," in *Proceedings of IFAC World Congress 2011*, Milan, Italy, August-September 2011, pp. 8316–8321.

[22] R. Moore, R. Kearfott, and M. Cloud, *Introduction to interval analysis*. Society for Industrial Mathematics, 2009.

[23] T. Alamo, J. Bravo, and E. Camacho, "Guaranteed state estimation by zonotopes," *Automatica*, vol. 41, no. 6, pp. 1035–1043, 2005.

[24] K. Østergaard, P. Brath, and J. Stoustrup, "Estimation of effective wind speed," in *Journal of Physics: Conference Series*, vol. 75. IOP Publishing, 2007, p. 012082.

[25] T. Knudsen, T. Bak, and M. Soltani, "Prediction models for wind speed at turbine locations in a wind farm," *Wind Energy*, 2011.